Manuscript version
DOI original paper: 10.1109/CDC45484.2021.9683098

Robust Control of Relative Degree Two Systems Subject to Output Constraints with Time-Varying Bounds

Mark Spiller and Dirk Söffker

***Abstract*— In this paper robust constrained control of nonlinear systems that have relative degree two with respect to the control variable is considered. The first time derivative of the control variable is assumed to be the constrained variable. The developed control approach is based on sliding mode control design. It places sliding manifolds below the bounds of the constraints so that the constrained variable will be forced to stay in the admissible region if it approaches a bound. For the proposed control method it is analytically shown that the constrained control problem can be solved. This includes consideration of time-varying behavior of the bounds. Velocity-constrained control of a two-link robot is considered as a numerical example.**

I. INTRODUCTION

Constrained control problems arise in many applications like autonomous vehicles, process industry, traffic control or robotics.

Model predicitve control (MPC) is widely applied and known for its property to handle constraints of MIMO systems. In addition to that MPC forecasts the future system behavior in order to minimize a defined performance index over the considered time horizon [1]. However, MPC is model-based which means that parametric- or external uncertainties may have a negative influence on the control performance. In order to overcome this problem several approaches related to robust MPC have been developed. The strategy behind the so-called min-max approaches is to minimize the performance index of MPC for the worst possible sequence of the disturbance [2]. The method is known to be computationally demanding and due to its conservative selection strategy it may lead to suboptimal performance results [3]. Scenario optimization [4], [5] is another robust MPC approach. A finite number of disturbance realizations is drawn from a known probability measure of the disturbance. The obtained finite number of realizations forms one scenario for which the performance index is minimized. Dependent on the number of disturbance realizations it can be determined how likely it is that the solution of the optimization problem indeed satisfies the constraints and reaches the terminal region. Tube based MPC is another robust control strategy. It guarantees the sytem states to remain in a tube around the nominal trajectory although some disturbances may be present [6]. The method was first proposed for linear systems [6] and later extended to nonlinear systems e. g. [7].

Sliding mode control (SMC) is well established in the field of nonlinear robust control [8]. It forces the system states on a manifold called sliding surface. The dynamics on the surface can be designed in order to achieve some desired behavior like convergence of tracking error. Disturbances within the range of defined uncertainty bounds are rejected by pushing the states back on the sliding surface immediately. This behavior of the SMC provides inherent robustness against parametric uncertainties and external disturbances. Compared to MPC the computational burden of SMC is less. The drawback of conventional SMC is a high frequency switching of the input signal denoted as chattering. In order to mitigate this effect several approaches have been develeoped e. g. the boundary layer approach [9], the exponential reaching law [10], [11], higher order SMCs [12], [13], and adaptive gain approaches [14], [15].

Several constrained SMC approaches can be found in the literature. The authors in [16] make use of a state transformation to express the constraints in terms of the sliding variables. A higher order SMC is applied to drive the sliding variables to zero without violating the constraints. A maximum domain of attraction is achieved and the approach can be applied to nonlinear systems with generic relative degree. In [17] similar results are achieved regarding constrained control of nonlinear relative degree two systems. A maximum domain of attraction is also provided. An approach denoted as sliding mode reference conditioning is proposed in [18]. It is an outer loop control approach that manipulates the reference signal of an already controlled system. Based on this manipulation the closed loop system is kept in a sliding mode that guarantees the constraints to be satisfied. The constraints can be formulated with respect to the closed loop states. Only bounds of the time derivatives of the closed loop states are required to be known for the controller design. The approach can also be applied to nonlinear systems. In [19] parameters of a linear time-varying sliding surface are optimized to achieve either input saturation or to satisfy velocity or acceleration constraints. The considered system has relative degree three. A similar approach based on a nonlinear sliding surface is proposed in [20] to achieve velocity-constrained control of relative degree two systems. In [21] the class of linear time-invariant systems with bounded disturbances is considered. A sliding mode controller is applied and robust positive invariant (RPI) sets of the closed loop dynamics are determined. The intersection of a state constraint set and the RPI set of the closed loop dynamics is studied. Conditions are derived for which the intersection itself is a RPI set. In [22] output constrained control of linear single input systems is considered. Multiple sliding mode controllers are combined with each other using

The authors are with the Chair of Dynamics and Control, University of Duisburg-Essen, Duisburg, 47057 Germany (e-mail: mark.spiller@uni-due.de, soeffker@uni-due.de)

a min-max selection strategy. The min-max selection scheme is a multi-controller approach known e. g. from aerospace industry where it is used for constrained turbo engine control [23]. Instead of linear controllers the approach of [22] applies SMCs within the framework. The approach proposed in [24] considers robust constrained control of nonlinear systems that satisfy the so-called conic sector constraint [25]. State feedback and SMC are combined in order to guarantee that the quadratic norm of the output variables does not exceed a defined threshold neither in the reaching phase nor in sliding mode. In [26] a time-varying nonlinear sliding mode is designed in order to achieve velocity-constrained control of relative degree two systems. For constrained control of linear time-invariant systems with bounded disturbances a SMC has been proposed in [27]. It considers input saturation and state constraints. The contribution [28] studies conditions under which polygonal state constraints are satisfied.

This paper considers robust constrained control of nonlinear systems that have relative degree two with respect to the control variable. The first time-derivative of the control variable is assumed to be constrained. The bounds of the constraints may explicitly depend on time. The developed control strategy is a multi-controller approach that combines sliding mode controllers. Sliding manifolds are placed below the bounds of the constraints and become active when the constrained variable approaches a bound. As a result the constrained variable is pushed away from the bound and kept in the admissible region. For the suggested approach it is mathematically shown that the constrained control problem can be solved. The novelty of the suggested method is its ability to handle bounds that explicitly depend on time. This is an extension of our previous work [29] which is restricted to time-invariant bounds and does only prove boundedness but not convergence of the tracking error. The aformention approach of [16] is general in the sense that it can handle any constraints expressed in terms of the sliding variables. However, it cannot handle time-varying bounds.

The paper is organized as follows. In Section II the constrained control problem is described and the assumptions are introduced. The control approach is developed and analyzed in Section III. Velocity-constrained robot control is considered as a numerical example in Section IV. Concluding remarks are made in Section V.

II. Problem Formulation

In this contribution the class of control-affine nonlinear relative degree two systems

$$\dot{\mathbf{x}} = f(\mathbf{x}) + g(\mathbf{x})u, \tag{1}$$

$$y_r = h(\mathbf{x}), \tag{2}$$

with states $\mathbf{x} \in \mathcal{X} \subseteq \mathbb{R}^n$, control variable $y_r \in \mathbb{R}$, and control input $u \in \mathbb{R}$ is addressed. Only y_r and its time derivative $\dot{y}_r$ are assumed to be available. A set-point tracking problem

$$\lim_{t\to\infty} y_r(t) = w, \tag{3}$$

with constant reference value $w \in \mathbb{R}$ is considered. The goal is to achieve set-point tracking in compliance with constraint

$$c_1: \quad y_{c_1}(t) = s_{c_1}\dot{y}_r(t) \le l_{c_1}(t), \qquad s_{c_1} = +1, \tag{4}$$

being defined by the upper bound $l_{c_1}(t)$ and constraint

$$c_2: \quad y_{c_2}(t) = s_{c_2}\dot{y}_r(t) \le l_{c_2}(t), \qquad s_{c_2} = -1, \tag{5}$$

being defined by the lower bound $-l_{c_2}(t)$. The bounds of the constrained variable $\dot{y}_r(t)$ may be time-varying i. e. $l_{c_i}(t) \in \mathbb{R}_{>0}$ but are assumed to be bounded from above. The input-output description

$$\ddot{y}_r = L_f^2 h(\mathbf{x}) + L_g L_f h(\mathbf{x})u, \tag{6}$$

with

$$\Psi = L_f^2 h(\mathbf{x}), \qquad \Gamma = L_g L_f h(\mathbf{x}), \tag{7}$$

is obtained from (1)–(2), where L_f and L_g denote the Lie derivatives. The uncertainty bounds

$$|\Psi| \le \Psi_M, \qquad 0 < \Gamma_m \le \Gamma \le \Gamma_M, \tag{8}$$

are assumed to be finite. The output constraints are connected to the sliding manifold

$$\sigma_{c_i}(t) = -\eta_{c_i}(t) + y_{c_i}(t) = 0, \qquad i \in \{1, 2\}, \tag{9}$$

with function $\eta_{c_i}(t)$ and constant $\eta_{m,c_i} \in \mathbb{R}_{>0}$ chosen as

$$\forall t: \quad 0 < \eta_{m,c_i} < \eta_{c_i}(t) < l_{c_i}(t). \tag{10}$$

Quantity $\eta_{c_i}(t)$ is assumed to be sufficient smooth

$$\max_t \left(|\dot{\eta}_{c_1}(t)|, |\dot{\eta}_{c_2}(t)|\right) < \dot{\eta}_M, \tag{11}$$

and to be bounded from below

$$0 < \eta_m < \min(\eta_{m,c_1}, \eta_{m,c_2}), \tag{12}$$

where $\eta_m, \dot{\eta}_M \in \mathbb{R}_{>0}$ are constant. The sliding variable σ_r is related to the tracking task and defines a linear sliding manifold

$$\sigma_r = -\dot{e}_r - a_0 e_r = \dot{y}_r - a_0 w + a_0 y_r = 0. \tag{13}$$

Quantity e_r denotes the tracking error

$$e_r = w - y_r. \tag{14}$$

and a_0 is a positive constant selected according to

$$a_0 \ge \frac{\dot{\eta}_M}{\eta_m} + \mu_a, \qquad \mu_a > 0, \tag{15}$$

with $\mu_a \in \mathbb{R}_{>0}$ being user-defined. It is assumed that $y_r = h(\mathbf{x})$ and $\dot{y}_r = L_f h(\mathbf{x})$ are continuous functions so that σ_r and σ_{c_i} are continuous.

III. Controller Design

The control design is separated into two parts. First, a conventional SMC is designed to solve the tracking problem. Second, an additional SMC is designed to drive the constrained variable to a sliding surface placed below the bounds of the constraints. If the constrained variable approaches a bound the additional SMC becomes active pushing the variable away from the bound. The transitions between the controllers can be made smooth by choosing a suitable controller structure.

In the following, a control law u_r is derived that solves the unconstrained set-point tracking task. Related to the reaching of the sliding manifold $\sigma_r = 0$, we introduce the Lyapunov function candidate $V_r = 0.5\sigma_r^2$. The dynamics

$$\dot{\sigma}_r = \Psi + \Gamma u_r + a_0 \dot{y}_r. \tag{16}$$

of the sliding variable σ_r are obtained by derivating (13) with respect to time and substituting (6). To ensure that V_r is indeed a Lyapunov function the control input u_r has to be selected suitably to guarantee that inequality

$$\begin{aligned} \dot{V}_r = \dot{\sigma}_r \sigma_r &= \Psi \sigma_r + \Gamma \sigma_r u_r + a_0 \dot{y}_r \sigma_r, \\ &\leq \Psi_M |\sigma_r| + a_0 \dot{y}_r \sigma_r + \Gamma \sigma_r u_r, \\ &\leq -\frac{\mu_r}{\sqrt{2}} |\sigma_r| < 0, \end{aligned} \tag{17}$$

is satisfied for $\sigma_r \neq 0$. Quantity $\mu_r \in \mathbb{R}_{>0}$ is a user-defined parameter that influences the rate of convergence. Dividing (17) by $|\sigma_r| > 0$ and $\Gamma > 0$ leads to

$$-\text{sgn}(\sigma_r) u_r \geq \frac{\mu_r + \Psi_M \sqrt{2}}{\Gamma_m \sqrt{2}} + \frac{a_0 \dot{y}_r \text{sgn}(\sigma_r)}{\Gamma}, \tag{18}$$

which is solved by

$$u_r = \begin{cases} -\text{sgn}(\sigma_r) \left(k_r + \frac{a_0 b |\dot{y}_r|}{\Gamma_m} \right), & \text{if } b \geq 0, \\ -\text{sgn}(\sigma_r) \left(k_r + \frac{a_0 b |\dot{y}_r|}{\Gamma_M} \right), & \text{if } b < 0, \end{cases} \tag{19}$$

$$k_r = \frac{\mu_r + \Psi_M \sqrt{2}}{\Gamma_m \sqrt{2}} + \frac{\dot{\eta}_M}{\Gamma_m}, \qquad b = \text{sgn}(\dot{y}_r \sigma_r). \tag{20}$$

Consequently, by applying control input u_r according to (19) function V_r is indeed a Lyapunov function that makes $|\sigma_r|$ decrease to zero in finite-time as stated by (17). The term $+\frac{\dot{\eta}_M}{\Gamma_m}$ of k_r is added as it becomes cruical in the proof of Lemma III.2 which shows that $\dot{y}_r$ will not approach the bound of constraint c_1 (c_2) if $\sigma_r > 0$ ($\sigma_r < 0$) holds.

In the following, an additonal control law u_{c_i} is designed to avoid violation of the constraints. From (9) it is known that the sliding manifold $\sigma_{c_i} = 0$ is placed below the bound of the constraint. Consequently, surface $\sigma_{c_i} = 0$ should be reached if y_{c_i} is too close to the bound l_{c_i}. Reaching of the manifold is considered based on the Lyapunov function candidate $V_{c_i} = 0.5\sigma_{c_i}^2$. The controller structure of the addional SMC is assumed as

$$u_{c_i} = u_r - s_{c_i} k_{c_i} \text{sgn}(\sigma_{c_i}). \tag{21}$$

Derivating (9) with respect to time and considering (4)–(6) leads to

$$\dot{\sigma}_{c_i} = -\dot{\eta}_{c_i} + s_{c_i} \Psi + s_{c_i} \Gamma u_{c_i}. \tag{22}$$

Multiplying (22) by σ_{c_i} yields

$$\begin{aligned} \dot{V}_{c_i} = \sigma_{c_i} \dot{\sigma}_{c_i} &= \sigma_{c_i} (s_{c_i} \Psi + s_{c_i} \Gamma u_{c_i} - \dot{\eta}_{c_i}), \\ &\leq -\frac{\mu_{c_i}}{\sqrt{2}} |\sigma_{c_i}| < 0, \end{aligned} \tag{23}$$

Algorithm 1 Robust Constrained Control Algorithm

Inputs $\sigma_{c_i}(t)$, $\sigma_r(t)$, $\eta_{c_i}(t)$, $y_{c_i}(t)$, $y_r(t)$
Parameters μ_{c_i}, μ_r, ϵ_{q_i}, ϵ_{c_i}, ϵ_r, ϵ_b, a_0, Ψ_M, Γ_m, Γ_M, $\dot{\eta}_M$
  $k_r \leftarrow \frac{\mu_r + \Psi_M \sqrt{2}}{\Gamma_m \sqrt{2}} + \frac{\dot{\eta}_M}{\Gamma_m}$
  if $\text{sgn}(\dot{y}_r \sigma_r) \geq 0$ **then**
    $u_{s,r} \leftarrow -\frac{\sigma_r}{|\sigma_r| + \epsilon_r} \left(k_r + \frac{a_0 \dot{y}_r \sigma_r |\dot{y}_r|}{(|\dot{y}_r \sigma_r| + \epsilon_b) \Gamma_m} \right)$
  else
    $u_{s,r} \leftarrow -\frac{\sigma_r}{|\sigma_r| + \epsilon_r} \left(k_r + \frac{a_0 \dot{y}_r \sigma_r |\dot{y}_r|}{(|\dot{y}_r \sigma_r| + \epsilon_b) \Gamma_M} \right)$
  end if
  if $\forall c_i : \sigma_{c_i} \leq 0$ **then**
    $u \leftarrow u_{s,r}$
  else if $\exists c_i : \sigma_{c_i} > 0$ **then**
    $p_{s,c_i} \leftarrow \frac{\mu_{c_i} + \Psi_M \sqrt{2}}{\Gamma_m \sqrt{2}} + \frac{\sigma_{c_i} s_{c_i}}{|\sigma_{c_i}| + \epsilon_{c_i}} u_r$
    if $-\dot{\eta}_{c_i} \text{sgn}(\sigma_{c_i}) \geq 0$ **then**
      $k_{s,c_i} \leftarrow p_{s,c_i} - \frac{\dot{\eta}_{c_i} \sigma_{c_i}}{|\dot{\eta}_{c_i} \sigma_{c_i}| + \epsilon_{q_i}} \frac{|\dot{\eta}_{c_i}|}{\Gamma_m}$
    else
      $k_{s,c_i} \leftarrow p_{s,c_i} - \frac{\dot{\eta}_{c_i} \sigma_{c_i}}{|\dot{\eta}_{c_i} \sigma_{c_i}| + \epsilon_{q_i}} \frac{|\dot{\eta}_{c_i}|}{\Gamma_M}$
    end if
    $u \leftarrow u_{s,r} - s_{c_i} k_{s,c_i} \frac{\sigma_{c_i}}{(|\sigma_{c_i}| + \epsilon_{c_i})}$
  end if
Output $u(t)$

where $\mu_{c_i} \in \mathbb{R}_{>0}$ is user-defined. Dividing (23) by $|\sigma_{c_i}| \neq 0$ gives

$$\text{sgn}(\sigma_{c_i})(s_{c_i} \Psi + s_{c_i} \Gamma u_{c_i} - \dot{\eta}_{c_i}) \leq -\frac{\mu_{c_i}}{\sqrt{2}}. \tag{24}$$

Rearranging and multiplying (24) by $-1/\Gamma < 0$ leads to

$$-\text{sgn}(\sigma_{c_i}) s_{c_i} u_{c_i} \geq \frac{\mu_{c_i}}{\Gamma \sqrt{2}} + \left(\frac{s_{c_i} \Psi}{\Gamma} - \frac{\dot{\eta}_{c_i}}{\Gamma}\right) \text{sgn}(\sigma_{c_i}). \tag{25}$$

From the uncertainty bounds (8), it follows

$$-\text{sgn}(\sigma_{c_i}) s_{c_i} u_{c_i} \geq \frac{\mu_{c_i} + \Psi_M \sqrt{2}}{\Gamma_m \sqrt{2}} - \frac{\dot{\eta}_{c_i}}{\Gamma} \text{sgn}(\sigma_{c_i}). \tag{26}$$

Substituting the controller structure (21) in (26) yields

$$k_{c_i} \geq \frac{\mu_{c_i} + \Psi_M \sqrt{2}}{\Gamma_m \sqrt{2}} - \frac{\dot{\eta}_{c_i}}{\Gamma} \text{sgn}(\sigma_{c_i}) + \text{sgn}(\sigma_{c_i}) s_{c_i} u_r, \tag{27}$$

which is required to be satisfied by the controller gain k_{c_i}. Finally, from (27) the control law

$$u_{c_1} = u_r - k_{c_1} \text{sgn}(\sigma_{c_1}), \tag{28a}$$
$$u_{c_2} = u_r + k_{c_2} \text{sgn}(\sigma_{c_2}), \tag{28b}$$

with

$$k_{c_i} = \begin{cases} p_{c_i} + \frac{\text{sgn}(q_{c_i}) |\dot{\eta}_{c_i}|}{\Gamma_m}, & \text{if } q_{c_i} \geq 0, \\ p_{c_i} + \frac{\text{sgn}(q_{c_i}) |\dot{\eta}_{c_i}|}{\Gamma_M}, & \text{if } q_{c_i} < 0, \end{cases} \tag{29}$$

$$q_{c_i} = -\dot{\eta}_{c_i} \text{sgn}(\sigma_{c_i}), \tag{30}$$

$$p_{c_i} = \frac{\mu_{c_i} + \Psi_M \sqrt{2}}{\Gamma_m \sqrt{2}} + \text{sgn}(\sigma_{c_i}) s_{c_i} u_r, \tag{31}$$

is obtained.

Both control laws (19) and (28) lead to chattering. To overcome the problem smooth approximations $\text{sgn}(a) \approx a/(|a|+\epsilon_a)$ with $\epsilon_a \in \mathbb{R}_{\geq 0}$ are introduced leading to

$$u_{s,r} = \begin{cases} -\frac{\sigma_r}{|\sigma_r|+\epsilon_r}\left(k_r + \frac{a_0 \dot{y}_r \sigma_r |\dot{y}_r|}{(|\dot{y}_r \sigma_r|+\epsilon_b)\Gamma_m}\right) & \text{if } b \geq 0, \\ -\frac{\sigma_r}{|\sigma_r|+\epsilon_r}\left(k_r + \frac{a_0 \dot{y}_r \sigma_r |\dot{y}_r|}{(|\dot{y}_r \sigma_r|+\epsilon_b)\Gamma_M}\right) & \text{if } b < 0, \end{cases} \quad (32)$$

with $\epsilon_r, \epsilon_b \in \mathbb{R}_{\geq 0}$ for (19) and

$$u_{s,c_i} = u_{s,r} - s_{c_i} k_{s,c_i} \frac{\sigma_{c_i}}{|\sigma_{c_i}|+\epsilon_{c_i}}, \quad (33)$$

with

$$k_{s,c_i} = \begin{cases} p_{s,c_i} + q_{s,c_i}\frac{|\dot{\eta}_{c_i}|}{\Gamma_m}, & \text{if } q_{c_i} \geq 0, \\ p_{s,c_i} + q_{s,c_i}\frac{|\dot{\eta}_{c_i}|}{\Gamma_M}, & \text{if } q_{c_i} < 0, \end{cases} \quad (34)$$

$$q_{s,c_i} = -\frac{\dot{\eta}_{c_i}\sigma_{c_i}}{|\dot{\eta}_{c_i}\sigma_{c_i}|+\epsilon_{q_i}}, \quad (35)$$

$$p_{s,c_i} = \frac{\mu_{c_i} + \Psi_M\sqrt{2}}{\Gamma_m\sqrt{2}} + \frac{\sigma_{c_i} s_{c_i}}{|\sigma_{c_i}|+\epsilon_{c_i}} u_r, \quad (36)$$

and $\epsilon_{c_i}, \epsilon_{q_i} \in \mathbb{R}_{\geq 0}$ for (28).

The overall control strategy is described as follows. From (4), (5), (9), (10) it can be seen that $\sigma_{c_i} \leq 0$ holds true if and only if the constrained variables are in the admissible region. In this case control law (32) is applied to achieve reference tracking. If $\sigma_{c_i} > 0$ holds the constrained variable is aproaching a bound so that control law (33) becomes active. It enforces $\sigma_{c_i} \leq 0$ so that violation of the constraints is avoided. The swichting between the controllers appears when σ_{c_i} switches from zero to a non-zero positive value and vice versa. Based on (33) it can be seen that $u_{s,c_i} \to u_{s,r}$ holds in case of $\sigma_{c_i} \to 0$. The transition of the controllers becomes smooth due to the chosen structure (21) and the applied smooth approximations of the signum function. The control strategy is summarized by Algorithm 1.

Based on the following analysis it is shown that the proposed controller solves the constrained control problem.

Theorem III.1. *Consider control of system (1)–(2) based on the control input defined by Algorithm 1 with $\epsilon_r = \epsilon_{c_i} = \epsilon_b = \epsilon_{q_i} = 0$. There exists some finite time t_f so that the constraints are satisfied for $t \geq t_f$ i. e.*

$$-l_{c_2}(t) \leq \dot{y}_r(t) \leq l_{c_1}(t), \quad (37)$$

holds for $t \geq t_f$. In addition $\sigma_{c_i}(t) \leq \Delta$ is achieved for $t \geq t_f$ with $\Delta > 0$ being arbitrary small. If $\forall c_i\colon \sigma_{c_i}(t_0) \leq 0$ holds for the initial time instant t_0 then $t_f = t_0$.

Proof. From Algorithm 1 it is known that the controller satisfies the reachability condition (23) in case of $\sigma_{c_i} > 0$. Consequently, $\sigma_{c_i}(t) < \Delta$ holds for $t \geq t_f$ with t_f being finite and $\Delta > 0$ being arbitrary small. Replacing Δ by some some specific $\tilde{\Delta}(t) = l_{c_i}(t) - \eta_{c_i}(t) > 0$ and considering the definition $\sigma_{c_i}(t) = -\eta_{c_i}(t) + y_{c_i}(t)$ leads to $y_{c_i}(t) < l_{c_i}(t)$ for $t \geq t_f$. ∎

Lemma III.2. *Consider control of system (1)–(2) based on the control input defined by Algorithm 1 with $\epsilon_r = \epsilon_{c_i} = \epsilon_b = \epsilon_{q_i} = 0$. Assume $\forall c_i\colon \sigma_{c_i}(t_{f1}) \leq 0$ to hold at some finite time t_{f1}. Then $\sigma_r(t)$ reaches zero at a finite time $t_{f2} \geq t_{f1}$. For $t \in [t_{f1}, t_{f2}]$ the value $|\sigma_r(t_{f1})|$ is an upper bound of $|\sigma_r(t)|$.*

Proof. The cases $\sigma_r(t_{f1}) > 0$ and $\sigma_r(t_{f1}) < 0$ are discussed separately.

Suppose $\sigma_r(t_{f1}) > 0$ to hold: It will first be shown that if $\sigma_r(t_{f1}) > 0$ and $\forall c_i : \sigma_{c_i}(t_{f1}) \leq 0$ hold then only input (19) or input (28b) are applied until σ_r reaches zero.

As $\forall c_i : \sigma_{c_i}(t_{f1}) \leq 0$ holds control input (19) is applied at time t_{f1}. Control input (19) is

$$u_r = -\left(k_r + \frac{a_0|\dot{y}_r|}{\Gamma_m}\right) < 0, \quad (38)$$

in case of $\sigma_r > 0$ and if $\dot{y}_r > 0$ is assumed. Replacing u_{c_i} in (22) by $u_r < 0$ from (38) and considering $\sigma_r > 0$ as well as assuming $\dot{y}_r > 0$ yields

$$\begin{aligned}\dot{\sigma}_{c_1} &= -\dot{\eta}_{c_i} + \Psi + \Gamma u_r, \\ &\leq \dot{\eta}_M + \Psi_M + \Gamma_m u_r = -\frac{\mu_r}{\sqrt{2}} - a_0|\dot{y}_r| < 0. \end{aligned} \quad (39)$$

If $\sigma_{c_1} = 0$ then $\dot{y}_r = \eta_{c_1} > 0$ holds and $\dot{y}_r$ is indeed positive. Consequently, (39) holds in case of $\sigma_{c_1} = 0$ guaranteeing that σ_{c_1} cannot become positive. Finally, as long as $\sigma_r > 0$ holds true and only control input (19) is applied $\sigma_{c_1} \leq 0$ holds.

Quantity σ_{c_2} may become positive so that the input changes to (28b). However, control input (28b) is only applied if $\sigma_{c_2} = -\eta_{c_2} - \dot{y}_r > 0$ holds which leads to $\sigma_{c_1} < -\eta_{c_1} - \eta_{c_2} < 0$. So $\sigma_{c_1} \leq 0$ holds true. Statement $\sigma_{c_1} \leq 0$ also holds if input (28b) switches to input (19). In this case $\sigma_{c_2} = -\eta_{c_2} - \dot{y}_r = 0$ holds which leads to $\sigma_{c_1} = -\eta_{c_1} - \eta_{c_2} < 0$. Consequently, input (28a) is not applied as long as $\sigma_r > 0$ holds.

It will be shown that by applying input (19) or (28b) sliding variable σ_r decreases to zero at finite time t_{f2} and $\sigma_r(t_{f1})$ is an upper bound of $\sigma_r(t)$ with $t \in [t_{f1}, t_{f2}]$. For input (19) the statement directly follows from the satisfied reachability condition (17) which implies that σ_r strictly decreases. Consider application of control input (28b). As $\forall c_i : \sigma_{c_i}(t_{f1}) \leq 0$ holds initially there may exist some instants of time $t_2 > t_1 > t_{f1}$ with $\sigma_{c_2}(t_1) = \sigma_{c_2}(t_2) = 0$. Consider $t^\dagger \in (t_1, t_2)$ to be a time interval in which $\sigma_{c_2}(t^\dagger) > 0$ holds. According to (13) it is

$$\sigma_r(t^\star) = \dot{y}_r(t^\star) - a_0 w + a_0 y_r(t_1) + \int_{t_1}^{t^\star} a_0 \dot{y}_r(\tau) d\tau, \quad (40)$$

at any time $t^\star \in [t_1, t_2]$. From $\sigma_{c_2}(t^\star) \geq 0$ it is known that $\dot{y}_r(t^\star) \leq -\eta_{c_2}(t^\star)$ holds leading to

$$\sigma_r(t^\star) \leq a_0(y_r(t_1) - w) + \int_{t_1}^{t^\star} a_0 \dot{y}_r(\tau) d\tau - \eta_{c_2}(t^\star). \quad (41)$$

Consider a_0 to be a positive constant defined as

$$a_0 = \frac{\dot{\eta}_M}{\eta_m} + \mu_a \geq \frac{\dot{\eta}_{c_2}(t)}{\dot{y}_r(t)} + \mu_a, \qquad \mu_a > 0. \quad (42)$$

Substituting the right hand side of (42) in (41) and solving the integral and considering that $\dot{y}_r$ is negative and bounded as $\dot{y}_r \leq -\eta_m < 0$ gives

$$\sigma_r(t^\star) \leq a_0(y_r(t_1) - w) - \mu_a \eta_m (t^\star - t_1) - \eta_{c_2}(t_1). \quad (43)$$

From $\sigma_{c_2}(t_1) = 0$ it is known that $-\eta_{c_2}(t_1) = \dot{y}_r(t_1)$ holds. Replacing $-\eta_{c_2}(t_1)$ in (43) and considering the definition of σ_r from (13) yields

$$\sigma_r(t^\star) \leq \sigma_r(t_1) - \mu_a \eta_m (t^\star - t_1), \qquad \mu_a \eta_m > 0. \quad (44)$$

Suppose $\sigma_r(t_f) < 0$ to hold: The proof is similar to the $\sigma_r(t_{f1}) > 0$ case. ∎

Lemma III.3. *Consider control of system (1)–(2) based on the control input defined by Algorithm 1 with $\epsilon_r = \epsilon_{c_i} = \epsilon_b = \epsilon_{q_i} = 0$. There exists some finite time t_f so that $\sigma_r(t_f) = 0$ holds and $\sigma_{c_i}(t) \leq \Delta$ is achieved for $t \geq t_f$ with $\Delta > 0$ being arbitrary small.*

Proof. As the controller satisfies the reachability condition (23) in case of $\exists c_i \colon \sigma_{c_i} > 0$ it is always possible to find some finite time t_{f1} at which $\forall c_i \colon \sigma_{c_i}(t_{f1}) \leq 0$ holds and $\forall c_i \colon \sigma_{c_i}(t) \leq \Delta$ is achieved for $t \geq t_{f1}$ with $\Delta > 0$ arbitrary small. By applying Lemma III.2 it follows that the finite time $t_f \geq t_{f1}$ exists at which $\sigma_r(t_f) = 0$ holds. ∎

Theorem III.4. *Consider control of system (1)–(2) based on the control input defined by Algorithm 1 with $\epsilon_r = \epsilon_{c_i} = \epsilon_b = \epsilon_{q_i} = 0$. There exists some finite time t_f so that for $t \geq t_f$ the tracking error $|e_r(t)|$ converges to the domain $\frac{|\sigma_r|_M}{a_0}$ asymptotically, where $|\sigma_r|_M > 0$ is arbitrary small.*

Proof. Based on Lemma III.3 it is known that a finite time t_f exists so that $\sigma_r(t_f) = 0$ holds and

$$\sigma_{c_i}(t) \leq \Delta, \quad (45)$$

with $\Delta > 0$ arbitrary small is achieved for $t \geq t_f$. Under the mentioned conditions it will be shown that $\sigma_r(t)$ remains bounded for $t \geq t_f$ until $\sigma_r(t)$ reaches zero again. If σ_r reaches zero it will again be bounded afterwards as the preliminary formulated conditions are again satisfied i. e. σ_r equals zero and (45) is satisfied. Consider an arbitray small $\epsilon > 0$ to be the maximum value of $|\sigma_r(t^*)|$ on some time interval $t^* \in [t_f, t_\epsilon]$.

Suppose $\sigma_{c_i}(t_\epsilon) \leq 0$ to hold true for c_1 and c_2: It follows from Lemma III.2 that σ_r reaches zero at some finite time $t_{f2} \geq t_f$. As stated by the Lemma $|\sigma_r|$ is bounded by $|\sigma_r(t_\epsilon)|$ on interval $[t_\epsilon, t_{f2}]$. As $|\sigma_r|$ is bounded by ϵ on interval $[t_f, t_\epsilon]$ it follows that $|\sigma_r|$ is bounded by arbitrary small $\epsilon \triangleq |\sigma_r|_M$ on interval $[t_f, t_{f2}]$.

Suppose $\sigma_{c_i}(t_\epsilon) > 0$ to hold true for c_1 exclusive or c_2: It will be shown that some finite time period τ_f exists so that $\sigma_{c_i}(t^\dagger) = -\eta_{c_i}(t^\dagger) + y_{c_i}(t^\dagger) \leq 0$ holds for $t^\dagger = t_\epsilon + \tau_f$ at the latest. As long as $\sigma_{c_i} > 0$ holds control input (28) is applied which satisfies the reachability condition $\sigma_{c_i}\dot{\sigma}_{c_i} \leq -\frac{\mu_{c_i}}{\sqrt{2}}|\sigma_{c_i}|$. For $\sigma_{c_i} > 0$ it follows

$$\dot{\sigma}_{c_i} = -\dot{\eta}_{c_i} + \dot{y}_{c_i} = -\dot{\eta}_{c_i} + s_{c_i}\ddot{y}_r \leq -\frac{\mu_{c_i}}{\sqrt{2}}. \quad (46)$$

As σ_{c_i} is known to be bounded by Δ according to (45) it follows that $\sigma_{c_i}(t_\epsilon + \tau_f) \leq 0$ can be achieved after the finite time period $\tau_f = \frac{\Delta\sqrt{2}}{\mu_{c_i}}$ at the latest. Since $\sigma_{c_i}(t_\epsilon + \tau_f) \leq 0$ holds Lemma III.2 can be applied and it is known that σ_r reaches zero at some finite time t_{f2}. Following the Lemma $|\sigma_r|$ is bounded by $|\sigma_r(t_\epsilon + \tau_f)|$ in interval $[t_\epsilon + \tau_f, t_{f2}]$. Boundedness in interval $[t_f, t_\epsilon + \tau_f]$ is studied as follows. Sliding variable $|\sigma_r|$ can only increase by applying input (28) (input (19) can only decrease $|\sigma_r|$). By applying the triangle inequality on (16) and considering the uncertainty bounds it follows

$$|\dot{\sigma}_r| = |\Psi + \Gamma u + a_0\dot{y}_r| \leq \Psi_M + \Gamma_M|u| + a_0 l_M, \quad (47)$$

with constant l_M defined as

$$\max_t \left(l_{c_1}(t), l_{c_2}(t)\right) < l_M. \quad (48)$$

Substituting (29)–(31) in (28) yields

$$u_{M,c_i} \triangleq \frac{\mu_{c_i} + \Psi_M\sqrt{2}}{\Gamma_m\sqrt{2}} + \frac{|\dot{\eta}_{c_i}|}{\Gamma_m} \geq |u_{c_i}|, \quad (49)$$

for input u_{c_i}. Substituting u of (47) by u_{M,c_i} from (49) gives

$$|\dot{\sigma}_r| \leq \frac{(\mu_{c_i} + \Psi_M\sqrt{2})\Gamma_M}{\Gamma_m\sqrt{2}} + \frac{|\dot{\eta}_{c_i}|\Gamma_M}{\Gamma_m} + \Psi_M + a_0 l_M \triangleq |\dot{\sigma}_r|_M. \quad (50)$$

Multiplying (50) by τ_f leads to

$$|\sigma_r(t^\S)| \leq |\dot{\sigma}_r|_M\tau_f + \epsilon, = \frac{|\dot{\sigma}_r|_M\sqrt{2}}{\mu_{c_i}}\Delta + \epsilon \triangleq |\sigma_r|_M, \quad (51)$$

for $t^\S \in [t_f, t_\epsilon + \tau_f]$. From (45) it is known that $\Delta > 0$ is arbitrary small. As $\Delta, \epsilon > 0$ in (51) are abitrary small it follows that $|\sigma_r|$ is bounded by $|\sigma_r|_M > 0$ arbitrary small on time interval $[t_f, t_\epsilon + \tau_f]$. Since $|\sigma_r|$ is bounded by $|\sigma_r(t_\epsilon + \tau_f)|$ on $[t_\epsilon + \tau_f, t_{f2}]$ as mentioned before it follows that $|\sigma_r|$ is bounded by $|\sigma_r|_M > 0$ arbitrary small on $[t_f, t_{f2}]$.

In the sequel it is shown that for $t \geq t_f$ the tracking error $|e_r(t)|$ converges to the domain $\frac{|\sigma_r|_M}{a_0}$ asymptotically. Consider $V(t) = |e_r(t)| > \frac{|\sigma_r|_M}{a_0}$ to hold. Derivating $V(t)$ with respect to time yields

$$\dot{V}(t) = \text{sgn}\left(e_r(t)\right)\dot{e}_r(t). \quad (52)$$

From (13) it is known that

$$-\dot{y}_r(t) = \dot{e}_r(t) = -a_0 e_r(t) - \sigma_r(t), \quad (53)$$

holds. In case of $|e_r(t)| > \frac{|\sigma_r|_M}{a_0}$ it follows

$$a_0|e_r(t)| > |\sigma_r|_M \geq |\sigma_r(t)|. \quad (54)$$

Based on (54) it can be seen that the sign of $-a_0 e_r(t) - \sigma_r(t)$ in (53) equals the sign of $-e_r(t)$. Consequently, if $|e_r(t)| > \frac{|\sigma_r|_M}{a_0}$ holds (53) can be written as

$$-\dot{y}_r(t) = \dot{e}_r(t) = -\text{sgn}(e_r(t))| - a_0 e_r(t) - \sigma_r(t)|, \quad (55)$$

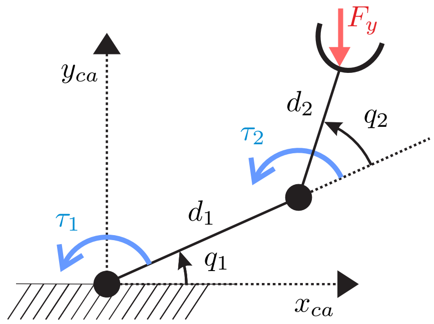

Fig. 1. Rotatory two-link robot with external force F_y, link lengths d_1 and d_2, joint angles q_1 and q_2, and torques τ_1 and τ_2.

with

$$|-a_0 e_r(t) - \sigma_r(t)| > 0. \tag{56}$$

Substituting (55) in (52) as well as (53) in (56) and considering that $\dot{y}_r(t)$ is bounded it follows

$$\dot{V}(t) = \begin{cases} -l_{c_1} < 0, & \text{if } \dot{y}_r = l_{c_1}, \\ -l_{c_2} < 0, & \text{if } -\dot{y}_r = l_{c_2}, \\ -1 \times |a| < 0, & \text{if } -l_{c_2} < \dot{y}_r < l_{c_1}, \end{cases} \tag{57}$$

$$|a| = |-a_0 e_r(t) - \sigma_r(t)| > 0,$$

in case of $V(t) = |e_r(t)| > \frac{|\sigma_r|_M}{a_0}$. Consequently, $|e_r(t)|$ converges to the domain $\frac{|\sigma_r|_M}{a_0}$ asymptotically. ■

IV. NUMERICAL EXAMPLE

In this section velocity-constrained point to point control of a robot is considered. Limitation of the robot velocity is known to be crucial in the context of safe human robot interaction [30]. The robot is assumed to be a rotatory two-link robot as shown in Fig. 1). The same kind of robot has been considered for constrained MPC in [31] and [32]. In [32] the two-link model has been used to implement MPC on a KUKA LWR IV. The dynamics of the two-link robot are given by

$$\mathbf{B}(\mathbf{q})\ddot{\mathbf{q}} + \phi(\mathbf{q}, \dot{\mathbf{q}}) = \tau + \xi(\mathbf{q}, F_y), \tag{58}$$

and

$$\phi(\mathbf{q}, \dot{\mathbf{q}}) = \mathbf{C}(\mathbf{q}, \dot{\mathbf{q}})\dot{\mathbf{q}} + f_v \dot{\mathbf{q}} + f_s \text{sgn}(\dot{\mathbf{q}}) + \mathbf{g}(\mathbf{q}), \tag{59}$$

where the joint angles, angular velocities, and actuator torques are

$$\mathbf{q} = \begin{bmatrix} q_1 \\ q_2 \end{bmatrix}, \qquad \dot{\mathbf{q}} = \begin{bmatrix} \dot{q}_1 \\ \dot{q}_2 \end{bmatrix}, \qquad \tau = \begin{bmatrix} \tau_1 \\ \tau_2 \end{bmatrix}. \tag{60}$$

The dynamics can be derived using Lagrange equations of the second kind [33]. Model (58) includes viscous friction f_v and static friction f_s. An external force F_y is considered to simulate a payload. The friction related quantities f_v and f_s as well as the payload are assumed unknown. Details about model (58 are given in Appendix I. The goal is to control the angles of the joints so that the end effector moves from an initial waypoint A (WP-A) to a waypoint C (WP-C) via an interim waypoint B (WP-B). During the movement the angular velocities of the joints are restricted. At WP-B a payload of 80 kg is picked up simulated by $F_y = 80\,\text{kg} \times 9.81\,\text{m/s}^2$. The Cartesian coordinates of the waypoints and their corresponding desired joint angles are shown in Table I. If the Euclidean distance between the actual and desired end effector position is less than $0.005\,\text{m}$ the robot moves to the next waypoint. If the last waypoint is reached with the desired accuracy the simulation terminates. Let $c_{i,j}$ define the i-th constraint of the angular velocity $\dot{q}_j$. The bound of the constraint $c_{i,j}$ is defined based on

TABLE I

CARTESIAN COORDINATES (x_{ca}, y_{ca}) AND JOINT ANGLES OF THE WAYPOINTS

	x_{ca} [m]	y_{ca} [m]	q_1 [°]	q_2 [°]
WP-A	0.900	0.100	26.511	−51.318
WP-B	−0.700	0.500	168.873	−62.720
WP-C	0.100	0.400	117.562	−136.817

$$l_{c_{i,j}} = \left(a_c(\text{WP}_{q_j} - q_j)^2 + b_c\right)\frac{2\pi}{360}, \quad i, j \in \{1, 2\}, \tag{61}$$

with $a_c = 26.26$, $b_c = 10$, and WP_{q_j} denoting the reference of angle q_j in radiant. The time-varying bound (61) enforces the robot to slow down when it approaches a waypoint.

To achieve the desired control goals the following MIMO controller

$$\tau = \mathbf{B}(\mathbf{q})\nu + \mathbf{C}(\mathbf{q}, \dot{\mathbf{q}})\dot{\mathbf{q}} + \mathbf{g}(\mathbf{q}), \tag{62}$$

with

$$\nu = \begin{bmatrix} \nu_1 & \nu_2 \end{bmatrix}^T, \tag{63}$$

is introduced. Substituting (62) in (58) yields

$$\ddot{y}_{r,1} = \Psi_1(\mathbf{q}, \dot{\mathbf{q}}, F_y) + \nu_1, \tag{64}$$

$$\ddot{y}_{r,2} = \Psi_2(\mathbf{q}, \dot{\mathbf{q}}, F_y) + \nu_2, \tag{65}$$

where Ψ_1, Ψ_2 denote uncertainties related to the unknown friction terms f_s, f_v, and the unknown payload F_y. The control problem is reduced to the design of two SISO controllers with relative degree two input-output relations. Algorithm 1 is applied to define the control inputs ν_1 and ν_2 separately. The controller parameters and uncertainty bounds are tuned by trial and error. The uncertainty bounds are increased until sufficient tracking performance is achieved. The boundary layer widths $\epsilon_a \in \mathbb{R}_{\geq 0}$ of the smooth approximations $\text{sgn}(a) \approx a/(|a| + \epsilon_a)$ are tuned to find a compromise between tracking accuracy and chattering mitigation. Let controller $j \in \{1, 2\}$ be related to the control of angle q_j. The auxiliary function $\eta_{c_i,j}(t)$ has to be chosen in accordance to (10). By adapting the difference $l_{c_i,j}(t) - \eta_{c_i,j}(t) > 0$ the distance between the constrained variables and their bounds can be adjusted. Function $\eta_{c_i,j}(t)$ is finally selected as

$$\eta_{c_i,j}(t) = l_{c_i,j}(t) - 4\frac{2\pi}{360}, \tag{66}$$

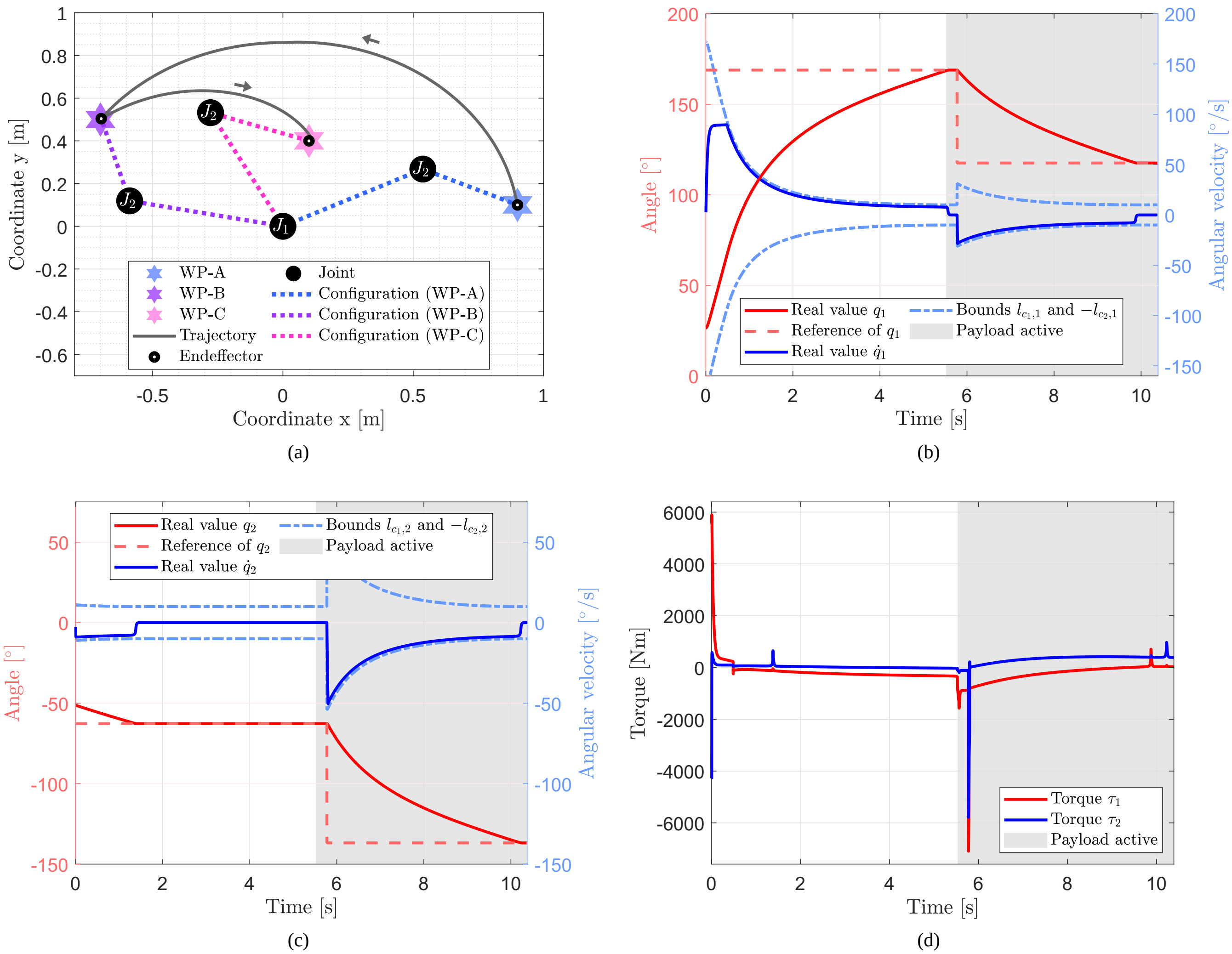

Fig. 2. Evaluation of control approach based on Algorithm 1. (a) Trajectory of the end effector in the Cartesian domain. Movement from WP-A to WP-C over WP-B. Visualization of robot configuration (joint angles) at the waypoints. (b) Angle and angular velocity of the first joint dependent on time. Visualization of reference value, constraints, and effect of the payload. (c) Angle and angular velocity of the second joint dependent on time. Visualization of reference value, constraints, and effect of the payload. (d) Torques generated by the controller. Visualization of rejection effect related to the payload.

for all $i, j \in \{1, 2\}$. The values of the remaining controller parameters are $\{\dot{\eta}_{M,j} = 6, \eta_{m,j} = 0.1, \mu_{a,j} = 0.01, \mu_{r,j} = 3, \mu_{c_i,j} = 2\}_{j=1}^{2}$. The assumed uncertainty bounds are $\Psi_M = 1$, $\Gamma_M = 2$, $\Gamma_m = 0.2$.

The simulation results are visualized in Fig. 2. The waypoints are reached with the desired accuracy and the velocity constraints are satisfied for the complete time horizon. The funnel shape of the velocity bounds forces the robot to slow down in the vicinity of a waypoint. The approach shows robust properties as the control goals are achieved in presence of model uncertainties and the unknown exogenous payload. A rejection effect related to the simulated payload can be observed from the control inputs.

V. CONCLUSIONS

In this contribution constrained sliding mode control is considered. As an extension to the existing works we presented a novel approach that can handle constraints which explicitly depend on time. This enables broader applications. Related to mechanical systems the suggested approach allows velocity-constrained control with online update of the velocity bounds depending on e. g. the distance to obstacles or set-points.

VI. ACKNOWLEDGMENTS

The authors want to thank the reviewers for their valueable comments.

REFERENCES

[1] J. B. Rawlings and D. Q. Mayne, *Model predictive control: Theory and design*. Nob Hill Pub., 2009.

[2] D. M. Raimondo, D. Limon, M. Lazar, L. Magni, and E. F. ndez Camacho, “Min-max model predictive control of nonlinear systems: A unifying overview on stability,” *European Journal of Control*, vol. 15, no. 1, pp. 5–21, 2009.

[3] A. Bemporad, F. Borrelli, and M. Morari, “Min-max control of constrained uncertain discrete-time linear systems,” *IEEE Transactions on Automatic Control*, vol. 48, no. 9, pp. 1600–1606, 2003.

[4] G. C. Calafiore and L. Fagiano, “Robust model predictive control via scenario optimization,” *IEEE Transactions on Automatic Control*, vol. 58, no. 1, pp. 219–224, 2012.

[5] G. Schildbach, L. Fagiano, C. Frei, and M. Morari, “The scenario approach for stochastic model predictive control with bounds on closed-loop constraint violations,” *Automatica*, vol. 50, no. 12, pp. 3009–3018, 2014.

[6] W. Langson, I. Chryssochoos, S. Raković, and D. Q. Mayne, “Robust model predictive control using tubes,” *Automatica*, vol. 40, no. 1, pp. 125–133, 2004.

[7] M. Cannon, J. Buerger, B. Kouvaritakis, and S. Rakovic, “Robust tubes in nonlinear model predictive control,” *IEEE Transactions on Automatic Control*, vol. 56, no. 8, pp. 1942–1947, 2011.

[8] Y. Shtessel, C. Edwards, L. Fridman, and A. Levant, *Sliding mode control and observation*. Springer, 2014.

[9] J.-J. E. Slotine, “Sliding controller design for non-linear systems,” *International Journal of Control*, vol. 40, no. 2, pp. 421–434, 1984.

[10] W. Gao and J. C. Hung, “Variable structure control of nonlinear systems: a new approach,” *IEEE Transactions on Industrial Electronics*, vol. 40, no. 1, pp. 45–55, 1993.

[11] C. J. Fallaha, M. Saad, H. Y. Kanaan, and K. Al-Haddad, “Sliding-mode robot control with exponential reaching law,” *IEEE Transactions on Industrial Electronics*, vol. 58, no. 2, pp. 600–610, 2010.

[12] A. Levant, “Higher-order sliding modes, differentiation and output-feedback control,” *International Journal of Control*, vol. 76, no. 9-10, pp. 924–941, 2003.

[13] F. Dinuzzo and A. Ferrara, “Higher order sliding mode controllers with optimal reaching,” *IEEE Transactions on Automatic Control*, vol. 54, no. 9, pp. 2126–2136, 2009.

[14] Y.-J. Huang, T.-C. Kuo, and S.-H. Chang, “Adaptive sliding-mode control for nonlinear systems with uncertain parameters,” *IEEE Transactions on Systems, Man, and Cybernetics, Part B (Cybernetics)*, vol. 38, no. 2, pp. 534–539, 2008.

[15] C. Edwards and Y. B. Shtessel, “Adaptive continuous higher order sliding mode control,” *Automatica*, vol. 65, pp. 183–190, 2016.

[16] G. P. Incremona, M. Rubagotti, and A. Ferrara, “Sliding mode control of constrained nonlinear systems,” *IEEE Transactions on Automatic Control*, vol. 62, no. 6, pp. 2965–2972, 2016.

[17] S. Ding, K. Mei, and S. Li, “A new second-order sliding mode and its application to nonlinear constrained systems,” *IEEE Transactions on Automatic Control*, vol. 64, no. 6, pp. 2545–2552, 2018.

[18] F. Garelli, R. J. Mantz, and H. d. Battista, *Advanced control for constrained processes and systems*. The Institution of Engineering and Technology, 2011.

[19] A. Bartoszewicz and A. Nowacka-Leverton, “ITAE optimal sliding modes for third-order systems with input signal and state constraints,” *IEEE Transactions on Automatic Control*, vol. 55, no. 8, pp. 1928–1932, 2010.

[20] M. Pietrala and M. Jaskuła, “IAE minimization in sliding mode control for second order systems with velocity constraint,” in *2019 20th International Carpathian Control Conference (ICCC)*. IEEE, 2019, pp. 1–6.

[21] H. Richter, B. D. O’Dell, and E. A. Misawa, “Robust positively invariant cylinders in constrained variable structure control,” *IEEE Transactions on Automatic Control*, vol. 52, no. 11, pp. 2058–2069, 2007.

[22] H. Richter, “A multi-regulator sliding mode control strategy for output-constrained systems,” *Automatica*, vol. 47, no. 10, pp. 2251–2259, 2011.

[23] J. Litt, D. Frederick, and T.-H. Guo, “The case for intelligent propulsion control for fast engine response,” *AIAA Infotech@Aerospace Conference*, pp. AIAA2009–1876, 2009.

[24] J. Song, Y. Niu, and Y. Zou, “Finite-time sliding mode control synthesis under explicit output constraint,” *Automatica*, vol. 65, pp. 111–114, 2016.

[25] M. N. ElBsat and E. E. Yaz, “Robust and resilient finite-time bounded control of discrete-time uncertain nonlinear systems,” *Automatica*, vol. 49, no. 7, pp. 2292–2296, 2013.

[26] M. Pietrala, M. Jaskula, and A. Bartoszewicz, “Terminal sliding mode control of second order systems with velocity constraint,” in *2018 19th International Carpathian Control Conference (ICCC)*. IEEE, 2018, pp. 223–227.

[27] M. Jaskuła and P. Leśniewski, “Constraining state variables and control signal via sliding mode control approach,” *IEEE Access*, vol. 8, pp. 111 475–111 481, 2020.

TABLE II

PARAMETERS OF TWO-LINK ROBOT [33]

b_1	131.5	$[\mathrm{kg\,m^2/rad}]$	b_2	6.0	$[\mathrm{kg\,m^2/rad}]$
b_3	13.0	$[\mathrm{kg\,m^2/rad}]$	b_4	3.0	$[\mathrm{kg\,m^2/rad}]$
b_5	112.0	$[\mathrm{kg\,m^2/rad}]$	c_1	3.0	$[\mathrm{kg\,m^2/rad^2}]$
g_1	309.0	$[\mathrm{kg\,m^2/s^2}]$	g_2	98.1	$[\mathrm{kg\,m^2/s^2}]$
f_v	0.2	$[\mathrm{kg\,m^2\,(s\,rad)^{-1}}]$	f_s	0.4	$[\mathrm{kg\,m^2/s^2}]$
d_1	0.6	$[\mathrm{m}]$	d_2	0.4	$[\mathrm{m}]$

[28] M. Innocenti and M. Falorni, “State constrained sliding mode controllers,” in *Proceedings of the 1998 American Control Conference*, vol. 1. IEEE, 1998, pp. 104–108.

[29] M. Spiller and D. Söffker, “Output constrained sliding mode control: A variable gain approach,” in *Proceedings of the 21th IFAC World Congress*. IFAC, 2020, in press.

[30] S. Haddadin, A. Albu-Schaffer, and G. Hirzinger, “The role of the robot mass and velocity in physical human-robot interaction part I: non-constrained blunt impacts,” in *2008 IEEE International Conference on Robotics and Automation*. IEEE, 2008, pp. 1331–1338.

[31] T. Faulwasser and R. Findeisen, “Nonlinear model predictive control for constrained output path following,” *IEEE Transactions on Automatic Control*, vol. 61, no. 4, pp. 1026–1039, 2015.

[32] T. Faulwasser, J. Matschek, P. Zometa, and R. Findeisen, “Predictive path-following control: concept and implementation for an industrial robot,” in *2013 IEEE International Conference on Control Applications (CCA)*. IEEE, 2013, pp. 128–133.

[33] B. Siciliano, L. Sciavicco, L. Villani, and G. Oriolo, *Robotics: modelling, planning and control*. Springer Science & Business Media, 2010.

APPENDIX I
SIMULATION OF ROBOTIC SYSTEM

According to [33] the quantities f_f, $\mathbf{B}$, $\mathbf{C}$, $\mathbf{g}$, ξ of model (58), (59) are

$$f_f(\dot{\mathbf{q}}) = f_v\dot{\mathbf{q}} + f_s\mathrm{sgn}(\dot{\mathbf{q}}), \tag{67}$$

$$\mathbf{B}(\mathbf{q}) = \begin{bmatrix} b_1 + b_2\cos(q_2) & b_3 + b_4\cos(q_2) \\ b_3 + b_4\cos(q_2) & b_5 \end{bmatrix}, \tag{68}$$

$$\mathbf{C}(\mathbf{q}, \dot{\mathbf{q}}) = -c_1\sin(q_2)\begin{bmatrix} \dot{q}_1 & \dot{q}_1 + \dot{q}_2 \\ -\dot{q}_1 & 0 \end{bmatrix}, \tag{69}$$

$$\mathbf{g}(\mathbf{q}) = \begin{bmatrix} g_1\cos(q_1) + g_2\cos(q_1 + q_2) \\ g_2\cos(q_1 + q_2) \end{bmatrix}, \tag{70}$$

$$\xi(\mathbf{q}, F_y) = F_y\begin{bmatrix} d_1\cos(q_1) + d_2\cos(q_1 + q_2) \\ d_2\cos(q_1 + q_2) \end{bmatrix}. \tag{71}$$

The position of the end effector in the Cartesian domain is

$$\mathbf{h}_{ca}(\mathbf{q}) = \begin{bmatrix} x_{ca} \\ y_{ca} \end{bmatrix} = \begin{bmatrix} d_1\cos(q_1) + d_2\cos(q_1 + q_2) \\ d_1\sin(q_1) + d_2\sin(q_1 + q_2) \end{bmatrix}. \tag{72}$$

The model parameters are summarized in Table II.